Food Research International 128 (2020) 108796

Contents lists available at ScienceDirect

Food Research International

journal homepage: www.elsevier.com/locate/foodres

Metabolic analysis of salicylic acid-induced chilling tolerance of banana using NMR

Lin Chen[a,c], Xue Zhao[a,c], Ji'en Wu[b], Yun He[a,c], Hongshun Yang[a,c,*]

[a] Department of Food Science & Technology, National University of Singapore, Singapore 117542, Singapore
[b] Setsco Services Pte., Ltd., Singapore 608925, Singapore
[c] National University of Singapore (Suzhou) Research Institute, 377 Lin Quan Street, Suzhou Industrial Park, Suzhou, Jiangsu 215123, PR China

ARTICLE INFO

Keywords:
Fruit
Metabolomics
Cold injury
Salicylic acid
Pathway
Energy status
Principal component analysis
Omics

ABSTRACT

Banana is highly susceptible to low temperature and salicylic acid (SA) can effectively improve the chilling tolerance. The metabolic changes of SA induced chilling responses of banana were studied. Bananas normally ripened under 15 °C and dramatic metabolic difference compared with other groups was recorded. Accumulation of glucose (> 1.5 folds) and consumption of unsaturated fatty acids (11.0–16.5%) were observed. The glycolysis was induced to compensate the decreased energy charge. Low temperature (6 °C) caused chilling damage and metabolites including glutamine, serine, and glucose were related to chilled bananas. Various physiological changes such as sugar metabolism and consumption of reducing substances occurred to adapt the cold stress. SA released the cold injury and the disaccharides were increased by 18.1–21.4%. Further analysis revealed the synthesis of unsaturated fatty acids, amino acids such as proline, and enhanced energy charge. Thus, SA increased the chilling tolerance via a number of different metabolic mechanisms.

1. Introduction

As a typical climacteric fruit, banana presents short shelf life and rapid softening after harvest. Low temperature storage is an effective strategy to reduce the metabolic and respiratory levels, and it maintains the quality and extends the shelf life of postharvest fruits and vegetables (Siddiqui, Chakraborty, Ayala-Zavala, & Dhua, 2011). However, banana fruit is highly susceptible to chilling injury (CI) when exposed to temperature lower than 13 °C (Huang, Jian, Jiang, Duan, & Qu, 2016). The typical CI symptoms include peel browning or blackening, and failure of normal ripening process (Luo et al., 2017). Furthermore, various physiological disorders such as membrane oxidation are induced by the cold stress. Accumulated evidence shows that energy status plays an important role to maintain the physiological functions of chilled fruits (banana, mango, pear, etc.) (Li, Limwachiranon, Li, Du, & Luo, 2016). Activities of energy metabolism enzymes (H^+-ATPase and Ca^{2+}-ATPase) in cold-stored banana continuously decrease, resulting in lower ATP content and energy charge (Li et al., 2016). These negative responses eventually reduce banana quality and consumer acceptability, resulting in substantial economic loss.

Salicylic acid (SA) is an endogenous plant signaling molecule that plays an important role to influence various physiological processes, including development, growth, and resistant responses to biotic and abiotic stresses (Raskin, 1992; Vlot, Dempsey, & Klessig, 2009). Previous studies reveal that pre- or post-harvest applications of SA effectively alleviate cold damage of fruits and vegetables (pineapples, sweet peppers, plums, pomegranates, etc.) stored under low temperature (Khademi, Ashtari, & Razavi, 2019). The cold resistance is induced by SA via different physiological and metabolic mechanisms. SA activates the antioxidant enzyme system such as ascorbate peroxidase and glutathione reductase, to scavenge the cold-induced reactive oxygen species (ROS) (Siboza, Bertling, & Odindo, 2017). Also, the heat shock proteins are induced by SA to maintain the cellular homeostasis (Han, Zuo, Wang, Dong, & Gao, 2017). In addition, the contents of polyamine and phenolics are improved in SA-treated fruits. Soaking treatment of banana fruit in 1 mM SA effectively alleviates the CI by maintaining the membrane integrity and improving the cellular antioxidant capacity (Khademi et al., 2019). However, the comprehensive metabolic responses of SA-induced cold resistance and the effect of exogenous SA on energy status of cold-stored banana remain unclear.

Emerging metabolomic techniques provide feasible strategies to monitor the overall metabolic alterations during different physiological activities of plants. For instance, the differential metabolites of ten new races of *Capsicum annuum* cv. serrano were screened by nuclear magnetic resonance (NMR) spectroscopy and the races were separated into two clusters based on the metabolomic fingerprints (formic acid, malic

* Corresponding author at: Department of Food Science & Technology, National University of Singapore, Singapore 117542, Singapore.
E-mail address: chmynghs@nus.edu.sg (H. Yang).

https://doi.org/10.1016/j.foodres.2019.108796
Received 2 September 2019; Received in revised form 31 October 2019; Accepted 1 November 2019
Available online 21 November 2019
0963-9969/

acid, citric acid, fumaric acid, galactose, sucrose, glucose, and fructose) (Villa-Ruano et al., 2019). Moreover, the distinctive flavonoid metabolism of soybean was unveiled by NMR-based metabolomics and the results showed that rutin and its precursor, quercetin-3-O-glucoside were featured in semiwild soybean *Glycine gracilis* (Yun et al., 2016). Indeed, the metabolic analysis of SA-induced chilling tolerance of banana may provide global insights to understand the chilling response and actively regulate the crop cold storage.

The aim of this study was to investigate the global metabolic changes of banana under cold stress and the metabolic responses of SA-induced chilling resistance. Banana fruit was treated by water and SA, and stored under low temperature. The metabolites were extracted from different groups after storage and identified by one-dimensional (1D) and two-dimensional (2D) NMR spectra. Principal component analysis (PCA) was conducted to screen the metabolites responsible for the variable discrimination. Orthogonal partial least squares discriminant analysis (OPLS-DA) and pathway analysis were further applied to clarify the metabolic pathway differences between selected pairwise groups. Moreover, the metabolic analysis was verified by checking energy status related adenylates.

2. Materials and methods

2.1. Plant material and treatment

Banana fruit (*Musa acuminate* cv. Kluai Khai, AA group) at the green mature stage was purchased from a local wholesale market in Singapore. The bananas were immediately transported to the lab and separated into individual fingers. Fingers which were uniform in size and free of physical injuries and infections were selected and randomly divided into four groups (each group contained around 50 individual fingers for three biological replicates of 15). Three groups were soaked in deionised (DI) water for 10 min and the left group was immersed in SA solution (1 mM, 10 min) (Khademi et al., 2019). The treated fruits were air dried at room temperature (24–26 °C) for 30 min. After that, one DI water treated group was sampled at day 0 (group I). Another water treated group was stored under 15 °C (II) and the left water (III) and SA (IV) treated groups were stored under 6 °C for 6 days. After the cold storage, the peels of the fruit in each treated group (triplicates of 15) were collected, cut into pieces, frozen and ground in liquid nitrogen, freeze-dried, and stored in liquid nitrogen for further metabolites extraction.

2.2. Preparation of banana extracts

The freeze-dried powder of each group (100 mg) was mixed with 1.5 mL methanol-d_4 (Cambridge Isotope Laboratories, Tewksbury, MA, USA). The mixtures were kept at −20 °C with continuous shaking overnight and centrifuged at 12,000*g* (4 °C) for 20 min. The collected supernatants were mixed with trimethylsilylpropanoic acid (TSP, dissolved in methanol-d_4, 10 mM) to a final concentration of 1 mM. The obtained supernatants (600 μL) were transferred into 5 mm magnetic tubes (Sigma-Aldrich, St. Louis, MO, USA) and immediately subject to NMR analysis. Three independent biological samples of each group were tested independently (Rosa et al., 2015).

2.3. NMR analysis of banana extracts

A NMR spectrometer (DRX-500, Bruker, Rheinstetten, Germany) with a frequency of 500.23 MHz was used to test the prepared banana samples (Zhao, Zhao, Wu, Lou, & Yang, 2019). The standard NOESY setting (noesypr1d) was applied to record the ^{1}H spectrum with a width of 10.0 ppm. The 1D spectra were obtained by 128 scans and an automatic pulse calculation experiment (pulsecal) was conducted to modify the 90° pulse length. For identification of metabolites, the standard 2D ^{1}H–^{13}C heteronuclear single quantum coherence (HSQC) spectroscopy of a representative banana peel (I) was recorded by the hsqcedetgpsisp2.3 setting. The ^{1}H signal was monitored in F2 channel with a width of 10.0 ppm and ^{13}C was recorded in F1 channel (180.0 ppm width) (Liu et al., 2017, 2018).

2.4. Spectra processing and analysis

The baseline and phase distortions of obtained 1D ^{1}H spectra were manually corrected by the software TopSpin 3.6.0 (Bruker). Furthermore, the metabolic peaks were identified by the 2D NMR spectrum using the PubChem Database (https://pubchem.ncbi.nlm.nih.gov/), Biological Magnetic Resonance Data Bank (http://www.bmrb.wisc.edu/), Madison Metabolomics Consortium Database (http://mmcd.nmrfam.wisc.edu/), Human Metabolome Database (http://www.hmdb.ca/), and related references (Yuan et al., 2017; Zhu, Yang, et al., 2018). The ^{1}H signal peaks in the range of 0.0–10.0 ppm were integrated and normalised to TSP peak area at 0.0 ppm. The methanol region ranging from 3.29 to 3.32 ppm was excluded. The region buckets (0.02 ppm width) were divided from the normalised spectra and the collected binned data were further analysed (Girelli et al., 2018).

The resulting dataset was imported into SPSS (IBM, Armonk, NY, USA) to conduct the hierarchical cluster analysis using average linkage and Pearson distance as similarity metric. In addition, the PCA of built dataset was tested by SIMCA software (version 13.0, Umetrics, Umeå, Sweden) (Zhao, Wu, Chen, & Yang, 2019). Based on the result of PCA score plots, the Euclidean distances (D_E), two-sample Hotelling's T^2 test (T^2), critical F value (F_c), and true F value (F_t) between the pairwise variables were calculated. The fold changes (FCs) and related *P* values of pairwise groups (I-II and I-III) were calculated from the binned data. The volcano plots were constructed based on the obtained results. Metabolites with a FC $>$ 1.5 and P $<$ 0.05 were screened and they were used to perform the enrichment pathway analysis by MetaboAnalyst 4.0 (http://www.metaboanalyst.ca/).

To further study the metabolic responses of SA-induced banana cold resistance, the OPLS-DA of pairwise groups III-IV was conducted (Bo et al., 2019). The color coded loading line was obtained to exhibit the discriminated metabolites between two groups. Furthermore, the most significant metabolites were screened by the variable importance in projection (VIP) analysis. The metabolites with VIP value $>$ 1 were further subject to the metabolic pathway analysis in MetaboAnalyst 4.0 and the further biological interpretations were discussed based on the Kyoto Encyclopedia of Genes and Genomes (KEGG) database (https://www.genome.jp/kegg/pathway.html) (Zhao et al., 2019).

2.5. Quantitative contents of adenylates in banana samples

The contents of ATP, ADP, and AMP in banana samples were quantitatively determined by high performance liquid chromatography (HPLC) method (Chen et al., 2018). The adenylates were extracted by grinding freeze-dried banana sample (100 mg) in 5 mL 0.5 M perchloric acid solution. The extract was centrifuged and 3 mL supernate was neutralised to around pH 6.8 using sodium hydroxide solution (1 M). After being diluted to 4 mL, the solution was filtered by a 0.45 μm filter and the prepared extract was stored under −20 °C until use. For the quantitative measurement, a HPLC system (Alliance 2695, Waters, MA, U.S.A.) with a UV detector was applied and 20 μL extract was injected into the system. Phosphate buffer (0.05 M) at pH 7.0 and acetonitrile were used as solvent A and B, respectively, to separate the adenylates at flow rate of 1 mL min^{-1} under 254 nm. The solvent B was linearly increased to 30% (v/v) in 20 min and hold for another 5 min before the next injection. The adenylate (ATP, ADP, and AMP) contents were calculated based on the external standard curve (0–10 μg mL^{-1}, R^2 $>$ 0.99) and the energy charge (EC) was determined by the following formula: $(C_{ATP} + 0.5 \times C_{ADP})/(C_{ATP} + C_{ADP} + C_{AMP})$. Three biological repliacates were tested.

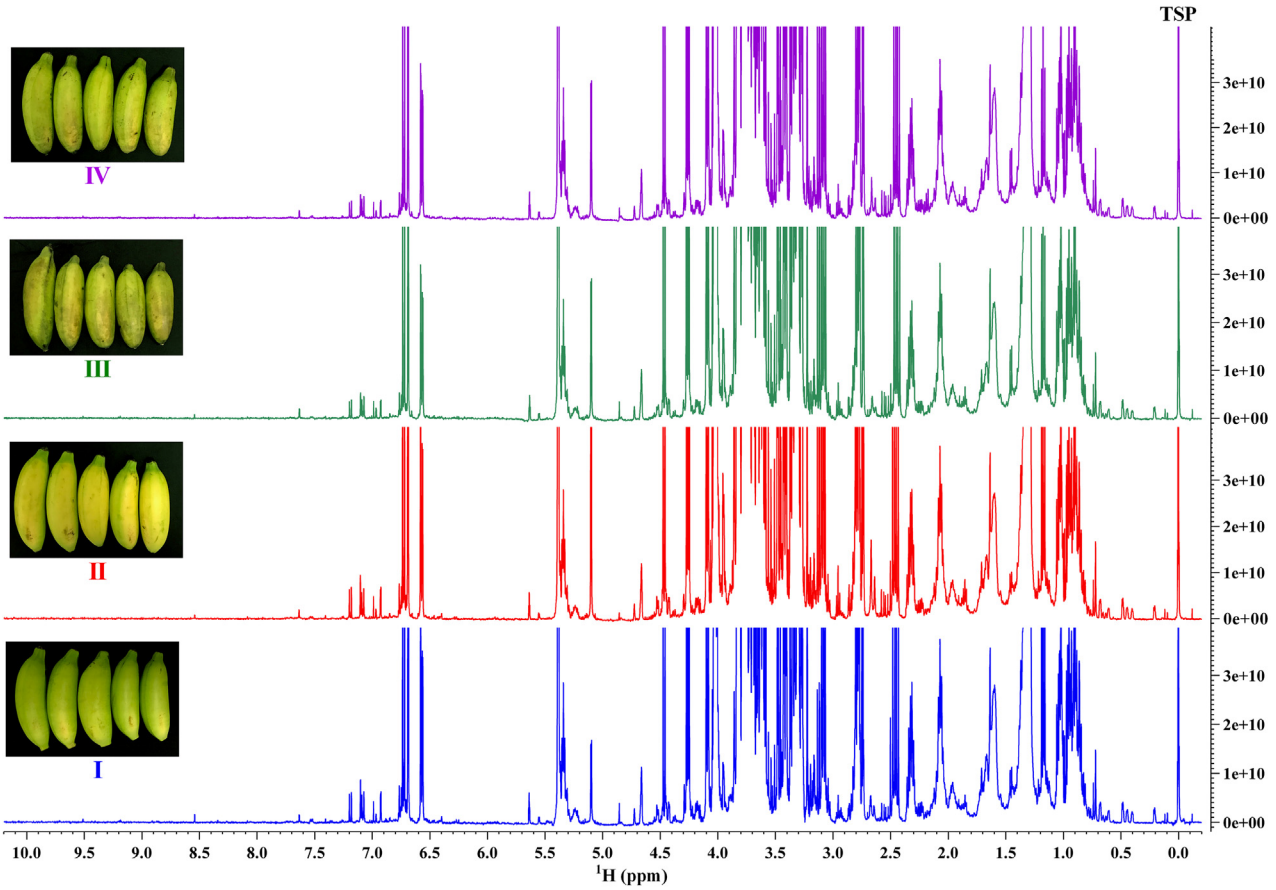

Fig. 1. ^{1}H spectra of banana samples. Note: I-IV represent banana before cold treatment, ripe banana stored under 15 °C for 6 days, banana stored under cold storage (6 °C) for 6 days, and salicylic acid treated banana stored under cold storage (6 °C) for 6 days, respectively.

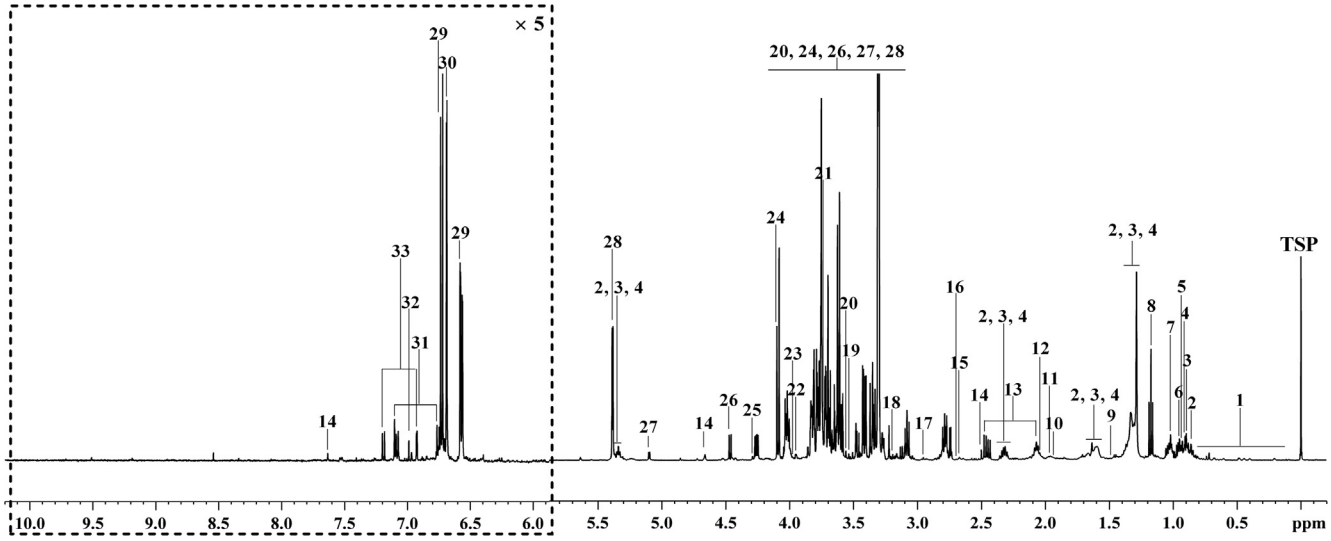

Fig. 2. Metabolic identification of representative banana peel extract. Note: 1, sterols; 2, linoleic acid; 3, oleic acid; 4, linolenic acid; 5, isoleucine; 6, leucine; 7, valine; 8, ethanol; 9, alanine; 10, γ-aminobutyric acid; 11, acetic acid; 12, proline; 13, glutamine; 14, pyridoxamine; 15, malic acid; 16, aspartic acid; 17, asparagine; 18, choline; 19, glycine; 20, maltose; 21, gluconic acid; 22, serine; 23, glycolic acid; 24, fructose; 25, ascorbic acid; 26, β-D-glucose; 27, α-D-glucose; 28, sucrose; 29, dopamine; 30, salsolinol; 31, phenolics; 32, gallic acid; 33, tyrosine.

2.6. Statistical analysis

Analysis of variance (ANOVA) was applied to analyse the obtained data statistically, and the mean values were compared by the least significant difference (LSD) method. Differences with P values < 0.05 were considered significant.

3. Results and discussion

3.1. Identification and comparison of metabolites in banana samples

The metabolic ^{1}H spectra of banana peels under different treatments (I-IV) are shown in Fig. 1. After storage of 6 days under 15 °C, green mature bananas (I) turned into yellow ripening (II) normally. Furthermore, the cold storage of 6 °C effectively delayed the ripening process (III and IV). However, severe CI occurred and the banana fruit exhibited browning peels (III). The SA treatment effectively alleviated the CI of banana (VI). These observations were in accordance with the results reported by Khademi et al. (2019) that SA treatment effectively decreased the chilling injury of banana by maintaining the membrane integrity and increasing the antioxidants. The ^{1}H results showed that the four spectra presented overall similar chemical shifts with different signal intensities, indicating similar chemical profiles of banana samples, but the contents of individual metabolites were varied. The major ^{1}H peaks were monitored at the region of 0.5–5.5 ppm (Fig. 1). Metabolites including sugars and aliphatic acids are typically assigned to this region (Chen et al., 2019). The results were in agreement with a previous study that banana peels are rich in polysaccharides (dietary fiber, starch, and soluble oligosaccharides), amino acids, and fatty acids (Emaga, Andrianaivo, Wathelet, Tchango, & Paquot, 2007). The detailed qualitative identification of 33 metabolic peaks and quantitative analysis of 30 identified metabolites without overlapping shifts were further performed based on the 2D spectrum and 1D binned area datasets, respectively (Fig. 2, Table 1).

Totally 33 compounds, including carbohydrates, unsaturated fatty acids, amino acids, and secondary metabolites, were identified in the representative banana peel sample (Fig. 2, Table S1). The ^{1}H signals in the region around 0.2–0.75 ppm represented the sterols, which are functional chemicals for human health (Yuan et al., 2017). In addition, sterols make up 11.1–28.0% of the total lipophilic components in banana pulp (Vilela et al., 2014). Various unsaturated fatty acids (linoleic acid, oleic acid, and linolenic acid) and free amino acids (isoleucine, valine, alanine, etc.) were identified in the region of 0.75–3.0 ppm. In the sugar region (3.0–5.5 ppm), soluble sugars including maltose, fructose, β-D-glucose, α-D-glucose, and sucrose were assigned. Furthermore, ^{1}H spectra indicated different contents of sugars in different groups. For example, α-D-glucose located at 5.13 ppm in ripe banana (II) presented highest signal intensity. The cold treated bananas (III and IV) also showed higher α-D-glucose contents compared with those before cold treatment (I) (Fig. 1). The induced glucose might provide reducing power to adapt to the cold stress (Yu, Shao, Wei, Xu, & Wang, 2017). Lastly, some ^{1}H signals in the region of 6.5–7.5 ppm indicated the existences of phenolic compounds including dopamine, salsolinol, and gallic acid in banana peels (Zhu, Yang, et al., 2018). These functional components are also rich in pulp tissues (Anyasi, Jideani, & Mchau, 2013, 2018).

Table 1 shows the quantitative contents of 30 identified metabolites in four banana groups. Linoleic acid, oleic acid, and linolenic acid constituted the major unsaturated fatty acids of banana peels and the results were in agreement with a previous study (Emaga et al., 2007). The contents of unsaturated fatty acids significantly ($P < 0.05$) decreased by 11.0–16.5% and 22.8–29.3% in group II and III, respectively, compared with I. The fatty acid characteristics in banana peel were similar with those in pulp reported by Khawas, Das, Sit, Badwaik, and Deka (2014). Linoleic and linolenic acids are the dominant unsaturated fatty acids and these lipophilic components present declining trends during the ripeness. Interestingly, SA treatment maintained the contents of three unsaturated fatty acids (Table 1). Recent studies revealed that sufficient linoleic and linolenic acids contribute to maintain

Table 1
The contents (mg g^{-1} DW) of identified metabolites in banana samples.

Metabolites		Banana groups (mg g^{-1} DW)			
		I	II	III	IV
2	Linoleic acid	8.34 ± 0.34 a	6.96 ± 0.14b	6.45 ± 0.10b	8.52 ± 0.84 a
3	Oleic acid	4.82 ± 0.13 a	4.29 ± 0.07b	3.83 ± 0.03c	4.84 ± 0.26 a
4	Linolenic acid	7.96 ± 0.18 a	6.79 ± 0.10b	6.48 ± 0.06c	8.29 ± 0.21 a
5	Isoleucine	6.41 ± 0.15 a	5.23 ± 0.11b	5.12 ± 0.15b	6.24 ± 0.11 a
6	Leucine	5.96 ± 0.17 a	5.23 ± 0.09b	4.79 ± 0.05c	5.90 ± 0.18 a
7	Valine	7.66 ± 0.16 a	6.92 ± 0.12b	6.43 ± 0.07c	7.60 ± 0.12 a
8	Ethanol	10.82 ± 0.22 a	6.81 ± 0.15b	3.68 ± 0.03c	2.57 ± 0.16 d
9	Alanine	0.62 ± 0.10 a	0.41 ± 0.20 a	0.53 ± 0.02 a	0.58 ± 0.19 a
10	γ-Aminobutyric acid	0.84 ± 0.08 a	0.71 ± 0.05 ab	0.66 ± 0.04b	0.79 ± 0.11 ab
11	Acetic acid	1.21 ± 0.06 a	1.10 ± 0.03b	0.92 ± 0.04c	1.18 ± 0.07 ab
12	Proline	1.75 ± 0.04b	1.51 ± 0.03c	1.34 ± 0.05 d	2.07 ± 0.11 a
13	Glutamine	2.66 ± 0.09c	3.98 ± 0.22b	5.93 ± 0.07 a	4.23 ± 0.13b
14	Pyridoxamine	2.66 ± 0.14 a	1.61 ± 0.05b	0.93 ± 0.06c	1.05 ± 0.06c
15	Malic acid	1.51 ± 0.01 d	4.07 ± 0.39 a	1.92 ± 0.10c	3.16 ± 0.04b
16	Aspartic acid	0.44 ± 0.04 a	0.33 ± 0.16 ab	0.23 ± 0.06c	0.31 ± 0.07 ab
17	Asparagine	1.07 ± 0.04b	1.58 ± 0.09 a	1.48 ± 0.05 a	1.17 ± 0.11b
18	Choline	0.44 ± 0.04 a	0.44 ± 0.04 a	0.27 ± 0.06b	0.32 ± 0.02b
19	Glycine	1.55 ± 0.04 d	2.66 ± 0.02 a	1.79 ± 0.09c	2.05 ± 0.02b
20	Maltose	2.36 ± 0.08 d	3.44 ± 0.04 a	2.56 ± 0.12c	2.89 ± 0.01b
22	Serine	2.20 ± 0.15 d	4.55 ± 0.01 a	3.85 ± 0.09c	4.10 ± 0.06b
23	Glycolic acid	2.25 ± 0.09 d	3.16 ± 0.01 a	2.46 ± 0.11c	2.90 ± 0.04b
24	Fructose	10.60 ± 0.30b	9.66 ± 0.07c	10.97 ± 0.14b	12.87 ± 0.06 a
25	Ascorbic acid	1.26 ± 0.21 a	1.56 ± 0.31 a	1.17 ± 0.11 a	1.21 ± 0.36 a
26	β-D-Glucose	6.65 ± 0.03 d	17.21 ± 0.30 a	10.20 ± 0.05b	8.39 ± 0.12c
27	α-D-Glucose	4.81 ± 0.10c	13.08 ± 0.24 a	7.51 ± 0.22b	7.61 ± 0.12b
28	Sucrose	18.47 ± 0.17b	15.75 ± 0.21c	18.78 ± 0.34b	21.81 ± 0.18 a
29	Dopamine	8.98 ± 0.25 a	8.30 ± 0.17b	5.94 ± 0.10 d	6.96 ± 0.12c
30	Salsolinol	10.14 ± 0.19 a	9.25 ± 0.14b	6.68 ± 0.06 d	7.81 ± 0.09c
32	Gallic acid	0.15 ± 0.02 ab	0.16 ± 0.00 a	0.12 ± 0.02c	0.13 ± 0.01 bc
33	Tyrosine	0.36 ± 0.01 a	0.37 ± 0.01 a	0.21 ± 0.01b	0.22 ± 0.01b

Within the same row, values with different lowercase letters are significantly different ($P < 0.05$). Note: I-IV represent banana before cold treatment, ripe banana stored under 15 °C for 6 days, banana stored under cold storage (6 °C) for 6 days, and salicylic acid treated banana stored under cold storage (6 °C) for 6 days, respectively.

the normal function of cellular membrane by preventing ion leakage and membrane lipid unsaturation (Shi et al., 2018). Thus, SA treatment might improve the chilling resistance of banana via inducing the synthesis of unsaturated fatty acids. Similarly, some amino acids such as isoleucine, leucine, and valine presented similar changing trends with the fatty acids (Table 1). Moreover, SA treatment even induced higher content of proline, which behaves like ROS scavenger (Yao, Xu, Farooq, Jin, & Zheng, 2018).

The sucrose in peel decreased from 18.47 to 15.75 mg g^{-1} dry weight (DW) during ripe process, while the contents of β-D-glucose and α-D-glucose were improved by 158.8% and 171.9%, respectively. The changing trends of sugars were similar with those in pulp tissue reported by Boudhrioua, Michon, Cuvelier, and Bonazzi (2002). The disaccharides such as sucrose in banana hydrolysis into small sugars (glucose and fructose) during storage. After cold storage (6 °C) of 6 days, the β-D-glucose and α-D-glucose contents in III increased by 53.4% and 56.1%, respectively, compared with those in group I. In addition, relative high contents of carbohydrates were recorded in SA treated group (Table 1). Accumulated reports evidence that sugar metabolism is involved in the chilling tolerance response and higher levels of related sugars such as sucrose, and reducing glucose and fructose account for higher chilling tolerance (Xu, Hu, Yang, & Jin, 2017). The obtained data indicated that SA treatment might improve the banana chilling tolerance via elevating contents of unsaturated fatty acids, related amino acids such as proline, and mono- and di-saccharides.

3.2. Hierarchical clustering and principal component analysis of the NMR dataset

The hierarchical clustering analysis was conducted based on the binned dataset of ^{1}H spectra (Fig. 3A). The results showed that the metabolic patterns of four groups were divided into two primary clusters: C1 and C2. C1 comprised group I, III, and IV, and group II was discriminative with the C1. The results indicated that cold storage maintained the major metabolic characteristics compared with the initial status before low temperature treatment. On the contrary, dramatic alterations of metabolic contents occurred during the ripening process of banana. Moreover, the subcluster C1a constituted by group III and IV indicated that cold storage resulted in some metabolic changes. Indeed, postharvest crops activate various transcriptional regulations and eventually modify the downstream metabolisms to survive under cold environment (Guo, Liu, & Chong, 2018).

PCA is a useful method to analyse multivariable groups and screen differential factors from high throughput data (Vong, Hua, & Liu, 2018). In the present work, the first three principal components (PCs) explained 95.9% of the whole data (PC1: 41.8%; PC2: 35.5%; PC3: 18.6%) and the high Q^2 value (0.91 $>$ 0.5) indicated a good predictive ability of the PCA model (Fig. 3B) (Liu et al., 2017). The score plots showed that samples from the same treatment were aggregated and the four groups were well separated (Fig. 3C). The metabolic profiles from group I and II were negatively influenced by PC1 and PC2, respectively (Table S2, Table S3). The Chilled banana group (III) was negatively affected by PC1 and PC2. In addition, SA treated group (IV) was positively influenced by PC3. The statistical tests including D_E and T^2 provide convincing quantitative metrics to compare the group separations. The tests showed D_E values ranging from 42.10 to 55.65 among the pairwise groups and the T^2 test exhibited that all the Ft values were larger than the Fc value, indicating significant separations of the variables (Fig. 3E).

The loading plots revealed the discriminative metabolites responsible for the variable separations (Fig. 3D). For examples, unsaturated fatty acids including linoleic acid, oleic acid, and linolenic acid were mainly affected by PC1 (Table S4, Table S5), indicating their close positive relationship with group I. In plants, fatty acids are vital cellular components, which provide structural basis of cell membrane and energy stock for physiological metabolism (Zhai et al., 2018). In addition, ethanol showed strong correlation with green mature banana (Table S2–S5) and it presented the highest content (10.82 mg g^{-1} DW) in group I (Table 1). Ethanol is considered to increase during the ripening and maturation of banana fruit (Zhu, Li, et al., 2018). It was increased from not detectable level to 0.92% in Brazilian banana fruit, but constantly not detected in Fenjiao banana at various ripening stages. The different results between our data and previous work may result from various factors such as different species, growth environment, harvesting time, etc. Glucose was positively associated with ripe banana stored under 15 °C. Sugar metabolism plays an important role during the postripeness of banana fruit (Yuan et al., 2017). Furthermore, fructose and sucrose were highly related to SA treated banana group (IV), agreeing with the conclusion that sucrose metabolism is involved in the chilling tolerance regulation (Xu et al., 2017). The sugars not only have osmoprotective function but also can induce the expression of cold response-related genes to alleviate the chilling damage.

3.3. Metabolic differences of pairwise groups I-II and I-III

To further understand the metabolic changes of banana fruit under low temperature storage (6 °C and 15 °C), the FCs of pairwise groups (I-II and I-III) were tested (Fig. 4A–C). Among the quantitative 30 metabolites in banana, the contents of 7 metabolites between group I and II were significantly different by over than 1.5 folds. Five metabolites including α-D-glucose, malic acid, β-D-glucose, serine, and glycine, presented higher contents in ripe banana (II) compared with the samples at green mature stage (I). On the contrary, ethanol and pyridoxamine showed higher concentrations in group I. During the ripening of banana, polysaccharides such as starch degrade into oligosaccharides or monosaccharides to provide substrates of energy producing (Nascimento et al., 2019; Yang et al., 2019). Also, malic acid is an important organic acid which involved in various metabolic pathways such as tricarboxylic acid cycle, glycolysis, gluconeogenesis, glyoxylate cycle and synthesis of secondary metabolites (Han et al., 2018). The induced contents of soluble sugars and related metabolites might contribute to compensate the energy deficit during ripening or senescence of banana, which was revealed by the study of He et al. (2017). The altered metabolic pathways of ripe banana under 15 °C were further investigated by enrichment pathway analysis (Fig. 4D, Table S6). Of the first ten metabolic pathways, five pathways were recognized as significantly altered with P values $<$ 0.05. The results showed that gluconeogenesis and glycolysis pathways were induced during the ripening process and the data further confirmed our hypothesis that higher energy production was required for group II. Furthermore, changes of ammonia recycling and methionine metabolism pathways showed the transformation of proteins and amino acids in banana by related enzymes.

The metabolic difference between group I and III was analysed to study the metabolic changes when CI occurred (Fig. 4B). The volcano plots showed higher contents of glutamine, serine, α-D-glucose, and β-D-glucose in chilled banana, while metabolites including ethanol, choline, tyrosine, phenolics, aspartic acid, and pyridoxamine were concentrated in group I. Further enrichment pathway analysis indicated that ammonia recycling, phosphatidylethanolamine biosynthesis, glycolysis, urea cycle, aspartate metabolism, and gluconeogenesis were involved to adapt the cold environment in banana (Fig. 4E, Table S7). He et al. (2017) reported that low temperature (7 °C) resulted in energy deficit and increase of membrane hydrolysis. The induced glucose and energy producing pathways (glycolysis and gluconeogenesis) of chilled banana by energy deficit in our results further confirmed that energy metabolism play a key role in responses to cold stress. Moreover, other physiological changes also occurred during the cold storage. For example, the choline was converted into some other metabolites in chilled banana (Table 1). In higher plants such as bean, barley, and rice, glycinebetaine is synthesised from choline in response to various

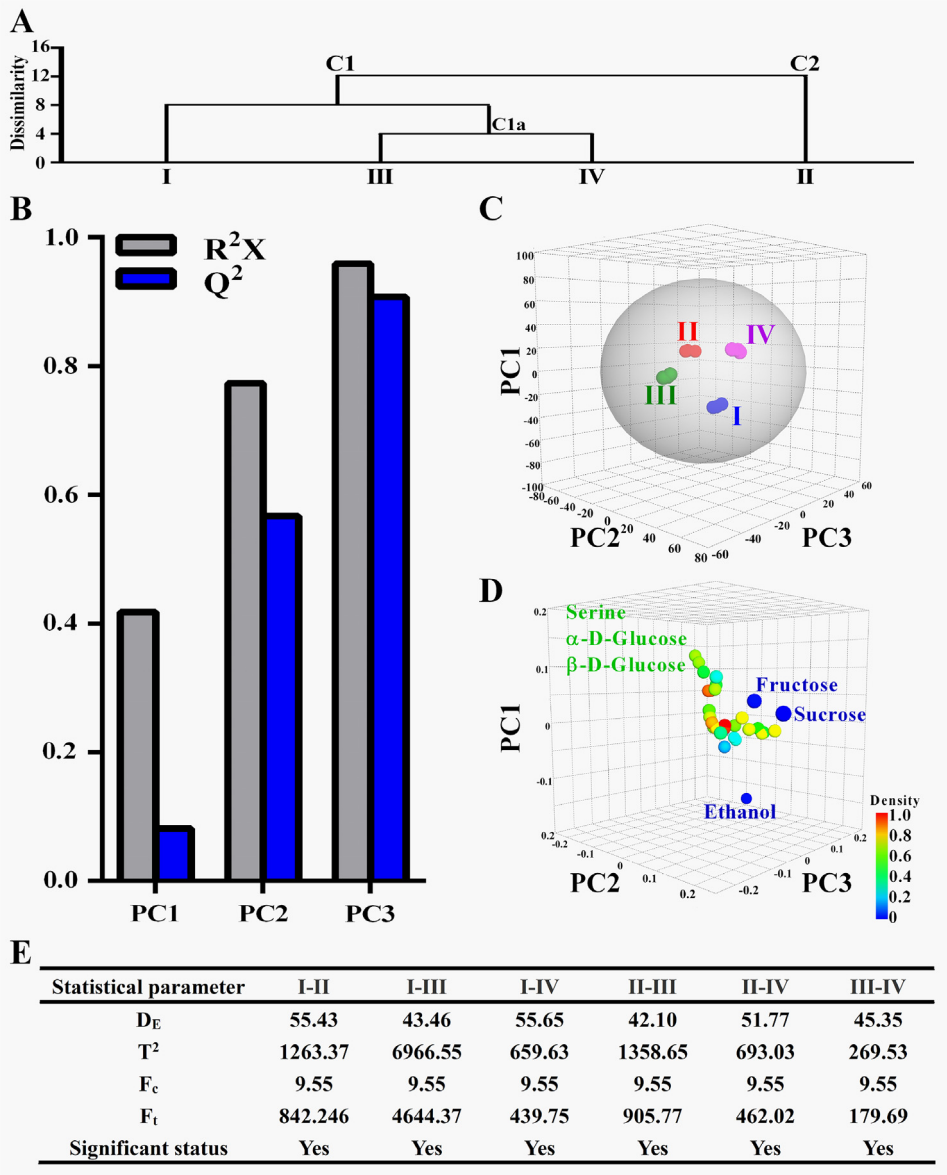

E

Statistical parameter	I-II	I-III	I-IV	II-III	II-IV	III-IV
D_E	55.43	43.46	55.65	42.10	51.77	45.35
T^2	1263.37	6966.55	659.63	1358.65	693.03	269.53
F_c	9.55	9.55	9.55	9.55	9.55	9.55
F_t	842.246	4644.37	439.75	905.77	462.02	179.69
Significant status	Yes	Yes	Yes	Yes	Yes	Yes

Fig. 3. Hierarchical cluster analysis of four groups (A); the principal components explaining variances used in principal component analysis (PCA) (B); the 3D score plots of PCA (C); the 3D loading plot of PCA (D); statistical analysis of variable separations (E). Note: I-IV represent banana before cold treatment, ripe banana stored under 15 °C for 6 days, banana stored under cold storage (6 °C) for 6 days, and salicylic acid treated banana stored under cold storage (6 °C) for 6 days, respectively.

environmental stresses (water, salt, and cold stresses) (Kurepin et al., 2017). Moreover, the reducing substrates such as phenolics and pyridoxamine were consumed during the banana CI (Table 1, Fig. 4C). ROS are accumulated in postharvest crops under cold stress and the plant has evolved various mechanisms to scavenge the oxidants. The consumption of non-enzymatic antioxidants such as phenolics is considered to balance the redox equilibrium when energy deficit occurred. For instance, the total phenolics content in DNP (2, 4-dinitrophenol, an inhibitor of ATP production) treated mung bean were significantly decreased by 15.39% because of the massive consumption during ROS scavenging (Chen, Tan, Zhao, Yang, & Yang, 2019).

3.4. Alterative metabolic profile of SA-induced chilling tolerance

The profile comparison of SA (IV) and DI water (III) treated banana fruit was conducted to investigate the overall metabolic alterations of SA-induced chilling tolerance (Fig. 5). The supervised OPLS-DA was applied to improve the quality of pairwise comparison (Chen et al., 2019). PC1 was the dominant factor (R^2: 0.99) to classify the variables and the results showed good separation of the two groups (Fig. 5A). Moreover, the Q^2 value of 0.99 indicated good fitness of the OPLS model (Chen et al., 2019). Furthermore, the loading S-line showed the discriminatory metabolites between the two groups. Metabolites with upward peaks indicated higher contents in SA treated group IV, while higher contents of metabolites in III presented downward peaks (Fig. 5B). In addition, the color-coded line presented the metabolite weights between the pairwise groups and the red color of metabolic signals exhibited notable differences (Liu et al., 2017, 2018). The further VIP test screened the significant metabolites contributed to the separation and 12 metabolites with VIP > 1 were considered as the significant compounds (Fig. 5C). Significant higher contents of sucrose, linolenic acid, malic acid, oleic acid, linoleic acid, proline, acetic acid, leucine and isoleucine were recorded in the group of IV. Moreover, the ethanol, β-D-glucose, and glutamine were considered as the significant factors of group III.

Pathway analysis was applied based on the screened metabolites to identify the most affected pathways involved in the SA-induced chilling tolerance. The result demonstrated that 18 pathways might be altered

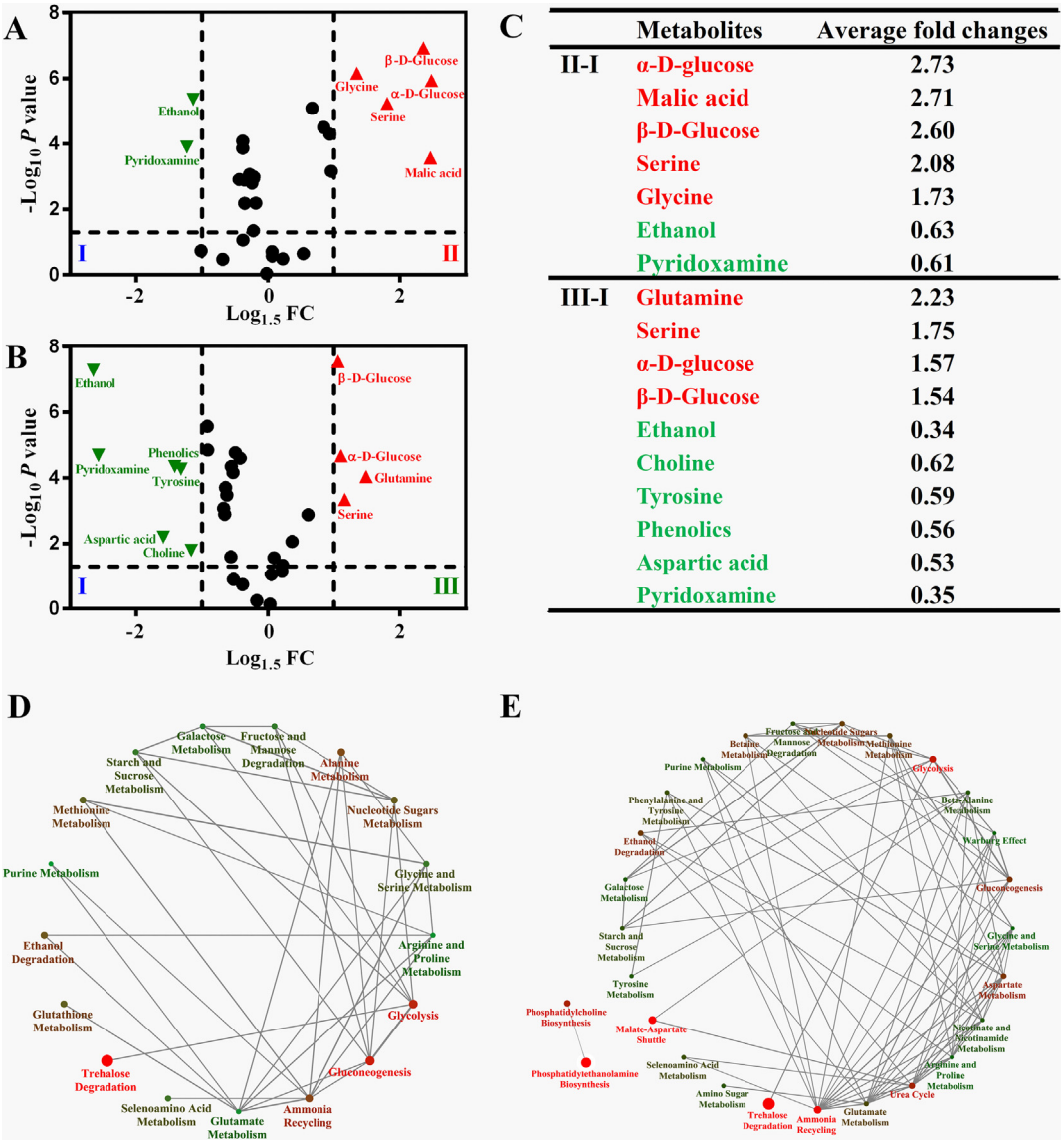

	Metabolites	Average fold changes
II-I	α-D-glucose	2.73
	Malic acid	2.71
	β-D-Glucose	2.60
	Serine	2.08
	Glycine	1.73
	Ethanol	0.63
	Pyridoxamine	0.61
III-I	Glutamine	2.23
	Serine	1.75
	α-D-glucose	1.57
	β-D-Glucose	1.54
	Ethanol	0.34
	Choline	0.62
	Tyrosine	0.59
	Phenolics	0.56
	Aspartic acid	0.53
	Pyridoxamine	0.35

Fig. 4. Volcano plots of screened metabolites in pairwise group I-II (A); volcano plots of screened metabolites in pairwise group I-III (B); average fold changes (FCs) of screened metabolites of pairwise groups (C); enrichment pathway analysis of pairwise group I-II (D); enrichment pathway analysis of pairwise group I-III (E). Note: I-IV represent banana before cold treatment, ripe banana stored under 15 °C for 6 days, banana stored under cold storage (6 °C) for 6 days, and salicylic acid treated banana stored under cold storage (6 °C) for 6 days, respectively.

by the SA treatment during cold storage (Fig. 5D, Table S8). Furthermore, 7 pathways (glycolysis or gluconeogenesis, aminoacyl-tRNA biosynthesis, biosynthesis of unsaturated fatty acids, valine, leucine and isoleucine biosynthesis, starch and sucrose metabolism, valine, leucine and isoleucine degradation, and arginine and proline metabolism) with $P < 0.05$ were regarded as the significant pathways. The results showed that SA treatment might alter the sugar metabolism and further change the energy status of chilled bananas. Liu et al. (2019) reported that fibroin treatment effectively alleviated chilling injury of banana by increasing the contents of mono- and di-saccharides and delaying the decreases in ATP and EC levels. In addition, the signal molecular SA induced the synthesis of unsaturated fatty acids and transformation of related amino acids such as proline to improve the chilling tolerance. The positive relationship between these metabolites with the cold tolerance of postharvest fruits and vegetables have been well studied. For example, the proline content in cold sensitive genetically modified (*SlCBF1* mutant) tomato was remarkably lower than the wild type, indicating the cold resistant function of proline (Li et al., 2018).

According to the screened metabolites, pathways, MetaboAnalyst 4.0 and KEGG databases, the reprograming biochemical pathways affected by SA treatment are summarised and illustrated in Fig. 5E. Under the cold stress, SA effectively elevated the contents of soluble sugars, such as sucrose and fructose, by inducing the degradation of starch or other polysaccharides. Moreover, SA resulted in the biosynthesis of unsaturated fatty acids. The accumulated unsaturated fatty acids contributed to the redox equilibrium by scavenging the ROS induced under cold stress. Furthermore, these metabolites (polysaccharides and fatty acids) also acted as energy source or stock for the normal physiological activities to prevent the CI of banana fruit. Changes of the amino acid metabolism were also induced by the SA treatment. Glutamine was converted into proline by related metabolic transformation. Overall, the SA treatment induced the chilling tolerance via different mechanisms including sugar, fatty acid, and amino acid.

3.5. Energy status of banana fruit under different treatments

To further confirm our hypothesis that SA altered the energy status to improve the chilling tolerance of cold stored bananas, the adenylates

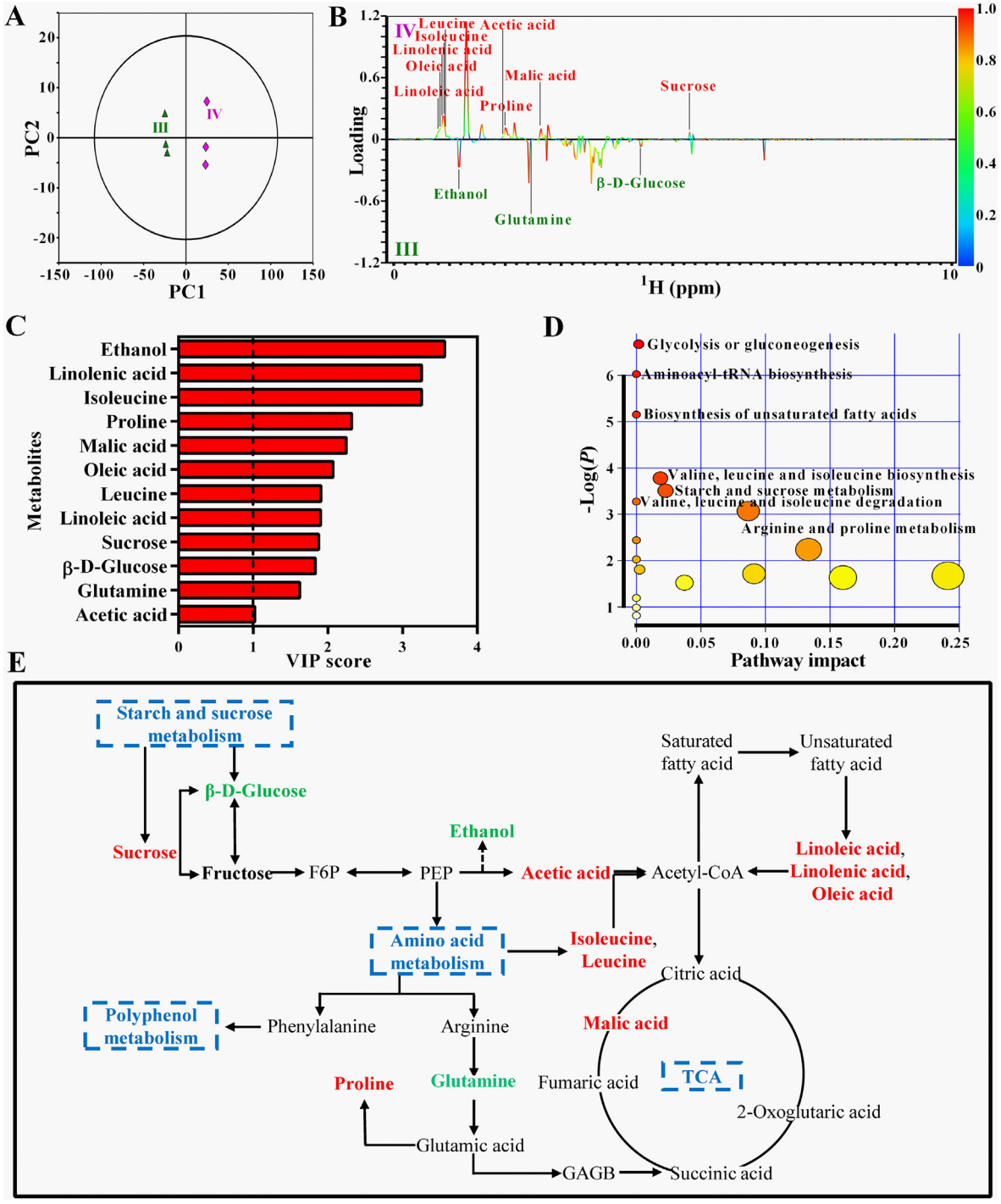

Fig. 5. Orthogonal partial least squares discriminant analysis (OPLS-DA) score plot of group III and IV, R^2 = 0.99, Q^2 = 0.99 (A); OPLS-DA loading S-line (B); screened metabolites with VIP > 1 (C); Overview of the pathway analysis of group III and IV (D); biochemical pathway analysis of SA-induced chilling tolerance, metabolites colored in red and green represent higher contents in IV and III, respectively (E). Note: I-IV represent banana before cold treatment, ripe banana stored under 15 °C for 6 days, banana stored under cold storage (6 °C) for 6 days, and salicylic acid treated banana stored under cold storage (6 °C) for 6 days, respectively. (For interpretation of the references to color in this figure legend, the reader is referred to the web version of this article.)

were quantitatively determined (Table 2). The normally ripened bananas presented significant lower EC compared with group I and the results agreed with a previous report that the EC of banana gradually decreased from around 0.8–0.5 during the long term (30 d) storage under 14 °C (He et al., 2017). In addition, ATP contents were significantly (P < 0.05) improved by 37.84% and 36.66% in low temperature treated groups III and IV, respectively (Table 2). ADP contents showed similar trends with ATP results. These data were in accord with the metabolic results that low temperature induced the glycolysis or gluconeogenesis pathway to activate the energy production. Previous results of cold stored mushroom showed similar results that low temperature maintained the quality by keeping higher energy level. The contents of ATP and ADP, and EC were significantly (P < 0.05) higher in 5 °C stored group compared with those in group stored under 10 °C (Zhang et al., 2019). Although the ATP contents in group III and IV were not significantly different, notably higher EC (0.83) was recorded

Table 2
Adenylate contents and energy charge (EC) of different banana groups.

Groups	Adenylates (mg 100 g^{-1} DW)			EC
	ATP	ADP	AMP	
I	72.73 ± 10.28 b	18.90 ± 1.25 c	12.60 ± 2.13 c	0.79 ± 0.06 ab
II	75.32 ± 9.65 b	20.36 ± 2.16 bc	25.28 ± 3.08 a	0.71 ± 0.02 c
III	100.25 ± 13.67 a	31.30 ± 5.17 a	15.79 ± 2.61 b	0.77 ± 0.02 b
IV	99.39 ± 11.17 a	23.55 ± 2.68 b	11.03 ± 1.15 c	0.83 ± 0.03 a

Within the same row, values with different lowercase letters are significantly different ($P < 0.05$). Note: I-IV represent banana before cold treatment, ripe banana stored under 15 °C for 6 days, banana stored under cold storage (6 °C) for 6 days, and salicylic acid treated banana stored under cold storage (6 °C) for 6 days, respectively.

in SA treated group (IV). The results indicated that the improved EC by SA treatment might contribute to the increased chilling tolerance of cold stored bananas.

4. Conclusion

In conclusion, this study investigated the metabolic alterations of SA-induced chilling tolerance of banana fruit using NMR. The obtained spectra results showed the metabolic differences among four groups. Bananas (group II) stored under 15 °C (6 d) were normally ripened and dramatic changes were recorded compared with initial status (I). Higher contents of monosaccharides were converted from polysaccharides, and the unsaturated fatty acids were consumed during the ripening process. Furthermore, the energy producing pathways were activated to compensate the low EC. Low temperature (6 °C) storage (group III) resulted in CI and the data analysis revealed that glutamine, serine, and glucose were closely related the chilled bananas. The glycolysis pathway was induced to keep the EC. SA treatment (group IV) effectively alleviated the CI of cold stored bananas and the PCA showed that fructose and sucrose were featured factors of IV. The supervised OPLS-DA indicated that SA induced higher contents of unsaturated fatty acids, disaccharides, and some amino acids such as proline via activating related metabolic pathways. Moreover, the SA improved the EC of cold stored bananas. These alterations cooperatively contributed to the enhanced chilling tolerance of banana.

Acknowledgement

This study was funded by the Singapore Ministry of Education Academic Research Fund Tier 1 (R-143-000-A40-114), Natural Science Foundation of Jiangsu Province (BK20181184), and an industry grant supported by Changzhou Qihui Management & Consulting Co., Ltd (R-143-000-A82-597).

Conflict of interest

We declare that we do not have any commercial or associative interest that represents a conflict of interest in connection with this manuscript. We have no financial and personal relationships with other people or organisations that can inappropriately influence our work.

Appendix A. Supplementary material

Supplementary data to this article can be found online at https://doi.org/10.1016/j.foodres.2019.108796.

References

Anyasi, T. A., Jideani, A. I., & Mchau, G. R. (2013). Functional properties and postharvest utilization of commercial and noncommercial banana cultivars. *Comprehensive Reviews in Food Science and Food Safety, 12*(5), 509–522.

Anyasi, T. A., Jideani, A. I., & Mchau, G. R. (2018). Phenolics and essential mineral profile of organic acid pretreated unripe banana flour. *Food Research International, 104*, 100–109.

Bo, Y., Feng, J., Xu, J., Huang, Y., Cai, H., Cui, X., ... Chen, Z. (2019). High-resolution pure shift NMR spectroscopy offers better metabolite discrimination in food quality analysis. *Food Research International, 125*, 108574.

Boudhrioua, N., Michon, C., Cuvelier, G., & Bonazzi, C. (2002). Influence of ripeness and air temperature on changes in banana texture during drying. *Journal of Food Engineering, 55*(2), 115–121.

Chen, L., Tan, G. J. T., Pang, X., Yuan, W., Lai, S., & Yang, H. (2018). Energy regulated nutritive and antioxidant properties during the germination and sprouting of broccoli sprouts (*Brassica oleracea* var. *italica*). *Journal of Agricultural and Food Chemistry, 66*(27), 6975–6985.

Chen, L., Tan, J. T. G., Zhao, X., Yang, D., & Yang, H. (2019). Energy regulated enzyme and non-enzyme-based antioxidant properties of harvested organic mung bean sprouts (*Vigna radiata*). *LWT-Food Science and Technology, 107*, 228–235.

Chen, L., Wu, J. E., Li, Z., Liu, Q., Zhao, X., & Yang, H. (2019). Metabolomic analysis of energy regulated germination and sprouting of organic mung bean (*Vigna radiata*) using NMR spectroscopy. *Food Chemistry, 286*, 87–97.

Emaga, T. H., Andrianaivo, R. H., Wathelet, B., Tchango, J. T., & Paquot, M. (2007). Effects of the stage of maturation and varieties on the chemical composition of banana and plantain peels. *Food Chemistry, 103*(2), 590–600.

Girelli, C. R., Accogli, R., Del Coco, L., Angilè, F., De Bellis, L., & Fanizzi, F. P. (2018). ^{1}H-NMR-based metabolomic profiles of different sweet melon (*Cucumis melo* L.) Salento varieties: Analysis and comparison. *Food Research International, 114*, 81–89.

Guo, X., Liu, D., & Chong, K. (2018). Cold signaling in plants: Insights into mechanisms and regulation. *Journal of Integrative Plant Biology, 60*(9), 745–756.

Han, C., Zuo, J., Wang, Q., Dong, H., & Gao, L. (2017). Salicylic acid alleviates postharvest chilling injury of sponge gourd (*Luffa cylindrica*). *Journal of Integrative Agriculture, 16*(3), 735–741.

Han, S., Nan, Y., Qu, W., He, Y., Ban, Q., Lv, Y., & Rao, J. (2018). Exogenous γ-aminobutyric acid treatment that contributes to regulation of malate metabolism and ethylene synthesis in apple fruit during storage. *Journal of Agricultural and Food Chemistry, 66*(51), 13473–13482.

He, X., Li, L., Sun, J., Li, C., Sheng, J., Zheng, F., ... Tang, Y. (2017). Adenylate quantitative method analyzing energy change in postharvest banana (*Musa acuminate* L.) fruits stored at different temperatures. *Scientia Horticulturae, 219*, 118–124.

Huang, H., Jian, Q., Jiang, Y., Duan, X., & Qu, H. (2016). Enhanced chilling tolerance of banana fruit treated with malic acid prior to low-temperature storage. *Postharvest Biology and Technology, 111*, 209–213.

Khademi, O., Ashtari, M., & Razavi, F. (2019). Effects of salicylic acid and ultrasound treatments on chilling injury control and quality preservation in banana fruit during cold storage. *Scientia Horticulturae, 249*, 334–339.

Khawas, P., Das, A. J., Sit, N., Badwaik, L. S., & Deka, S. C. (2014). Nutritional composition of culinary *Musa* ABB at different stages of development. *American Journal of Food Science and Technology, 2*(3), 80–87.

Kurepin, L. V., Ivanov, A. G., Zaman, M., Pharis, R. P., Hurry, V., & Hüner, N. P. (2017). Interaction of glycine betaine and plant hormones: Protection of the photosynthetic apparatus during abiotic stress. *Photosynthesis: Structures, mechanisms, and applications* (pp. 185–202). Cham: Springer.

Li, D., Limwachiranon, J., Li, L., Du, R., & Luo, Z. (2016). Involvement of energy metabolism to chilling tolerance induced by hydrogen sulfide in cold-stored banana fruit. *Food Chemistry, 208*, 272–278.

Li, R., Zhang, L., Wang, L., Chen, L., Zhao, R., Sheng, J., & Shen, L. (2018). Reduction of tomato-plant chilling tolerance by CRISPR-Cas9-mediated *SlCBF1* mutagenesis. *Journal of Agricultural and Food Chemistry, 66*(34), 9042–9051.

Liu, J., Li, F., Li, T., Yun, Z., Duan, X., & Jiang, Y. (2019). Fibroin treatment inhibits chilling injury of banana fruit via energy regulation. *Scientia Horticulturae, 248*, 8–13.

Liu, Q., Wu, J. E., Lim, Z. Y., Aggarwal, A., Yang, H., & Wang, S. (2017). Evaluation of the metabolic response of *Escherichia coli* to electrolysed water by ^{1}H NMR spectroscopy. *LWT-Food Science and Technology, 79*, 428–436.

Liu, Q., Wu, J. E., Lim, Z. Y., Lai, S., Lee, N., & Yang, H. (2018). Metabolite profiling of *Listeria innocua* for unravelling the inactivation mechanism of electrolysed water by nuclear magnetic resonance spectroscopy. *International Journal of Food Microbiology, 271*, 24–32.

Luo, D., Ba, L., Shan, W., Kuang, J., Lu, W., & Chen, J. (2017). Involvement of WRKY transcription factors in abscisic-acid-induced cold tolerance of banana fruit. *Journal of Agricultural and Food Chemistry, 65*(18), 3627–3635.

Nascimento, T. P., Castro-Alves, V. C., Castelan, F. P., Calhau, M. F. N., Saraiva, L. A., Agopian, R. G., & Cordenunsi-Lysenko, B. R. (2019). Metabolomic profiling reveals

that natural biodiversity surrounding a banana crop may positively influence the nutritional/sensorial profile of ripe fruits. *Food Research International, 124*, 165–174.
Raskin, I. (1992). Role of salicylic acid in plants. *Annual Review of Plant Biology, 43*(1), 439–463.
Rosa, A., Atzeri, A., Deiana, M., Scano, P., Incani, A., Piras, C., & Marincola, F. C. (2015). Comparative antioxidant activity and ^{1}H NMR profiling of Mediterranean fruit products. *Food Research International, 69*, 322–330.
Shi, F., Zhou, X., Zhou, Q., Tan, Z., Yao, M. M., Wei, B. D., & Ji, S. J. (2018). Membrane lipid metabolism changes and aroma ester loss in low-temperature stored Nanguo pears. *Food Chemistry, 245*, 446–453.
Siboza, X. I., Bertling, I., & Odindo, A. O. (2017). Enzymatic antioxidants in response to methyl jasmonate and salicylic acid and their effect on chilling tolerance in lemon fruit [*Citrus limon* (L.) Burm. F.]. *Scientia Horticulturae, 225*, 659–667.
Siddiqui, M. W., Chakraborty, I., Ayala-Zavala, J. F., & Dhua, R. S. (2011). Advances in minimal processing of fruits and vegetables: A review. *Journal of Scientific and Industrial Research, 70*, 823–834.
Vilela, C., Santos, S. A., Villaverde, J. J., Oliveira, L., Nunes, A., Cordeiro, N., ... Silvestre, A. J. (2014). Lipophilic phytochemicals from banana fruits of several *Musa* species. *Food Chemistry, 162*, 247–252.
Villa-Ruano, N., Ramírez-Meraz, M., Méndez-Aguilar, R., Zepeda-Vallejo, L. G., Álvarez-Bravo, A., Pérez-Hernández, N., & Becerra-Martínez, E. (2019). ^{1}H NMR-based metabolomics profiling of ten new races from *Capsicum annuum* cv. serrano produced in Mexico. *Food Research International, 119*, 785–792.
Vlot, A. C., Dempsey, D. M. A., & Klessig, D. F. (2009). Salicylic acid, a multifaceted hormone to combat disease. *Annual Review of Phytopathology, 47*, 177–206.
Vong, W. C., Hua, X. Y., & Liu, S. Q. (2018). Solid-state fermentation with *Rhizopus oligosporus* and *Yarrowia lipolytica* improved nutritional and flavour properties of okara. *LWT-Food Science and Technology, 90*, 316–322.
Xu, X. X., Hu, Q., Yang, W. N., & Jin, Y. (2017). The roles of cell wall invertase inhibitor in regulating chilling tolerance in tomato. *BMC Plant Biology, 17*(1), 195.
Yang, J., Zhu, H., Tu, J., Jiang, Y., Zeng, J., & Yang, B. (2019). Icariin as a preservative to maintain the fruit quality of banana during postharvest storage. *Food and Bioprocess Technology, 12*(10), 1766–1775.
Yao, W., Xu, T., Farooq, S. U., Jin, P., & Zheng, Y. (2018). Glycine betaine treatment alleviates chilling injury in zucchini fruit (*Cucurbita pepo* L.) by modulating antioxidant enzymes and membrane fatty acid metabolism. *Postharvest Biology and Technology, 144*, 20–28.
Yu, L., Shao, X., Wei, Y., Xu, F., & Wang, H. (2017). Sucrose degradation is regulated by 1-methycyclopropene treatment and is related to chilling tolerance in two peach cultivars. *Postharvest Biology and Technology, 124*, 25–34.
Yuan, Y., Zhao, Y., Yang, J., Jiang, Y., Lu, F., Jia, Y., & Yang, B. (2017). Metabolomic analyses of banana during postharvest senescence by ^{1}H-high resolution-NMR. *Food Chemistry, 218*, 406–412.
Yun, D., Kang, Y., Yun, B., Kim, E., Kim, M., Park, J. S., ... Hong, Y. (2016). Distinctive metabolism of flavonoid between cultivated and semiwild soybean unveiled through metabolomics approach. *Journal of Agricultural and Food Chemistry, 64*(29), 5773–5783.
Zhai, Z., Keereetaweep, J., Liu, H., Feil, R., Lunn, J. E., & Shanklin, J. (2018). Trehalose 6-phosphate positively regulates fatty acid synthesis by stabilizing WRINKLED1. *The Plant Cell, 30*(10), 2616–2627.
Zhang, Z., Zhang, X., Xin, G., Gong, X., Wang, Y., Wang, L., & Sun, B. (2019). Umami taste and its association with energy status in harvested *Pleurotus geesteranus* stored at different temperatures. *Food Chemistry, 279*, 179–186.
Zhao, L., Zhao, X., Wu, J. E., Lou, X., & Yang, H. (2019). Comparison of metabolic response between the planktonic and air-dried *Escherichia coli* to electrolysed water combined with ultrasound by ^{1}H NMR spectroscopy. *Food Research International, 125*, 108607.
Zhao, X., Wu, J. E., Chen, L., & Yang, H. (2019). Effect of vacuum impregnated fish gelatin and grape seed extract on metabolite profiles of tilapia (*Oreochromis niloticus*) fillets during storage. *Food Chemistry, 293*, 418–428.
Zhao, X., Zhou, Y., Zhao, L., Chen, L., He, Y., & Yang, H. (2019). Vacuum impregnation of fish gelatin combined with grape seed extract inhibits protein oxidation and degradation of chilled tilapia fillets. *Food Chemistry, 294*, 316–325.
Zhu, X., Li, Q., Li, J., Luo, J., Chen, W., & Li, X. (2018). Comparative study of volatile compounds in the fruit of two banana cultivars at different ripening stages. *Molecules, 23*(10), 2456.
Zhu, H., Yang, J., Jiang, Y., Zeng, J., Zhou, X., Hua, Y., & Yang, B. (2018). Morin as a preservative for delaying senescence of banana. *Biomolecules, 8*(3), 52.